Philippine Engineering Journal (1996) XVII (2): 53 - 66

ELASTO-PLASTIC SOIL-STRUCTURE ANALYSIS BY BEM-FEM SUBSTRUCTURE METHOD

Mark A. Zarco, Ph.D.
Associate Professor and Chairman
Department of Engineering Sciences
College of Engineering
University of the Philippines
Diliman, Quezon City, Philippines

and

Thangavelu Kuppusamy, Ph.D.
Professor and Head, Geotechnical Division
Charles Via Department of Civil Engineering
Virginia Polytechnic Institute and State University
Blacksburg, Virginia, USA

ABSTRACT

A method for solving soil-structure interaction problems which includes the infinite boundary effects of the far field domain is developed. The method involves coupling boundary elements based on the Melan fundamental solution with finite elements in a manner so as to result in a system of equations which is both symmetric and banded. Analyses of nonlinear soil-structure interaction problems such as bearing capacity, lateral earth pressure and U-frame lock construction problems are performed to investigate the far field domain effect.

INTRODUCTION

Soil-structure interaction problems involve the solution of boundary value problems involving two domains. A near field finite domain consisting of the structure and the soil adjacent to it, and a semi-infinite far field domain representing the soil distant from the structure. Because such problems normally involve complex geometry, boundary conditions and constitutive behavior, they must be solved numerically.

A number of researchers have coupled the boundary element and finite element method to solve problems involving a non-linear finite domain imbedded within an infinite linear domain. The concept of coupling the boundary element and finite element method is described in Zienkiewicz, Kelley and Bettes [141, and Johnson and Nedelec [7]. The main setback of coupling the boundary element to the finite element method is that the symmetry and bandedness of the stiffness matrix resulting from the finite element method is destroyed due to the boundary element method. Numerous researchers (Jirousek and Teoderescu, [6]; Zielinski and Zienkiewicz, [13]) have tried to remedy the problem of unsymmetry by developing alternative boundary element formulations that produce a symmetric stiffness matrix. Nevertheless, the resulting element stiffness matrix when assembled into the global stiffness matrix destroys the latter's bandedness.

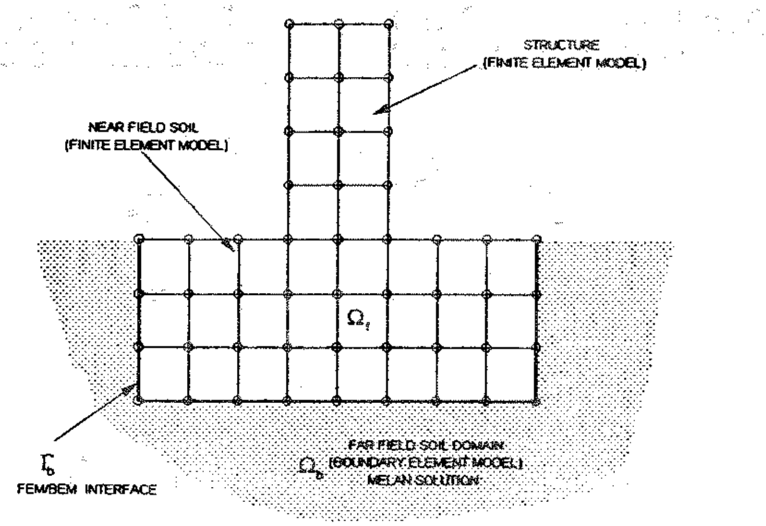

Figure 1. A typical soil-structure interaction problem modeled using the proposed boundary element-finite element model.

In the present study, a method for coupling the boundary element and finite element method in such a way as to preserve both the symmetry and bandedness is developed. This method is implemented into a computer program BEFEC, and a number of soil-structure interaction problems are solved to investigate the effects of domain size, finite element type, boundary conditions as well as the infinite boundary effects on the displacements and stresses predicted.

COUPLED BEM-FEM METHOD

The application of the coupled boundary element-finite element method to the solution of soil-structure interaction problems was first presented by Brebbia and Georgiou [2], and later by Vallabhan, et. al. [10]. In these two studies, the structure is modelled using finite elements, while the foundation soil is modelled using boundary elements based on the Kelvin solution. Because of the manner in which the foundation soil is modelled, these approaches are limited to linear problems where the far field domain is ignored. In the proposed coupled boundary element-finite element method for soil-structure interaction problems, the near field is modelled using 4-node isoparametric elements, while the far field is modelled using boundary elements based on the Melan Solution, as described by Telles and Brebia [9], assuming a linear and homogenous far-field domain. Using this approach, the non-linear and nonhomogenous nature of the soil in the near field domain can be modelled at the same time taking into consideration the effects of the infinite far-field domain. Figure 1 shows how a typical soil-structure interaction problem is modelled using the proposed method. The technique for coupling the boundary element and finite element method shall now be described. For elastostatic problems, the finite element results in a system of linear equations of the form:

$$\mathbf{KU} = \mathbf{F} \tag{1}$$

where $\mathbf{K}$ is the finite element stiffness matrix which is both symmetric and banded, $\mathbf{U}$ and $\mathbf{F}$ are the vectors of nodal displacements and forces respectively. For elastostatic problems involving half-plane domains, the direct boundary element method results in a system of equations of the form:

$$\mathbf{H}^M \hat{\mathbf{U}} = \mathbf{G}^M \hat{\mathbf{P}} \tag{2}$$

where $\mathbf{H}^M$ and $\mathbf{G}^M$ are matrices of influence coefficients based on the Melan fundamental solution, and $\hat{\mathbf{U}}$ and $\hat{\mathbf{P}}$ are the vectors of nodal boundary displacements and tractions respectively. Multiplying both sides of equation (2) by $\left(\mathbf{G}^M\right)^{-1}$ yields:

$$\left(\mathbf{G}^M\right)^{-1} \mathbf{H}^M \hat{\mathbf{U}} = \hat{\mathbf{P}} \tag{3}$$

The nodal boundary tractions are transformed linearly into nodal boundary forces by:

$$\hat{\mathbf{F}} = \mathbf{M}\hat{\mathbf{P}} \tag{4}$$

where $\mathbf{M}$ is a square matrix. Multiplying both sides of equation 3 by $\mathbf{M}$ yields:

$$\mathbf{M}\left(\mathbf{G}^M\right)^{-1} \mathbf{H}^M \hat{\mathbf{U}} = \hat{\mathbf{F}} \tag{5}$$

which can be rewritten in the form:

$$\hat{\mathbf{K}}\hat{\mathbf{U}} = \hat{\mathbf{F}} \tag{6}$$

where $\mathbf{K} = \mathbf{M}\left(\mathbf{G}^M\right)^{-1} \mathbf{H}^M$ can be viewed as an equivalent stiffness matrix for the boundary element system. This matrix is both asymmetric and fully populated.

To assemble the equivalent boundary element stiffness matrix into the finite element stiffness matrix in such a way as to preserve the bandedness of the system, the finite element system described in equation 1 must first be assembled such that the resulting system is partitioned in the following manner:

$$\left[\begin{array}{c|c} \mathbf{K}_{ff} & \mathbf{K}_{fb} \\ \hline \mathbf{K}_{bf} & \mathbf{K}_{bb} \end{array}\right] \left\{\begin{array}{c} \mathbf{U}_f \\ \hline \mathbf{U}_b \end{array}\right\} = \left\{\begin{array}{c} \mathbf{F}_f \\ \hline \mathbf{F}_b \end{array}\right\} \tag{7}$$

where $\mathbf{U}_b$ and $\mathbf{F}_b$ are the vectors of nodal displacements and forces respectively corresponding to nodes located along the interface of the boundary and finite element system, while $\mathbf{U}_f$ and $\mathbf{F}_f$ are the vectors of nodal displacements and forces respectively corresponding to nodes exclusive to the finite element domain. The nodal displacements and forces along the interface of the boundary and finite element system are related by compatibility and equilibrium which requires that:

$$\mathbf{U}_b = \hat{\mathbf{U}} \tag{8}$$

$$\mathbf{F}_b + \hat{\mathbf{F}} = 0 \tag{9}$$

Applying equations (6) and (7) through (9) yields:

$$\begin{bmatrix} \mathbf{K}_{ff} & \mathbf{K}_{fb} \\ \mathbf{K}_{bf} & \widetilde{\mathbf{K}}_{bb} \end{bmatrix} \begin{Bmatrix} \mathbf{U}_f \\ \mathbf{U}_b \end{Bmatrix} = \begin{Bmatrix} \mathbf{F}_f \\ \mathbf{F}_b \end{Bmatrix} \tag{10}$$

where

$$\widetilde{\mathbf{K}}_{bb} = \mathbf{K}_{bb} + \hat{\mathbf{K}} \tag{11}$$

Because the fully populated and asymmetric matrix $\hat{\mathbf{K}}$ is isolated to the bottom right-hand side corner, the resulting global stiffness matrix in equation (10) remains banded. It should also be noted that only the sub -matrix $\widetilde{\mathbf{K}}_{bb}$ becomes asymmetric. Thus, aside from the upper triangular portion of the global stiffness matrix, only the elements of $\widetilde{\mathbf{K}}_{bb}$ located beneath the principal diagonal need to be stored. Because the number of nodes located along the interface between the boundary element and finite element system is small compared to the total number of nodes, the additional computer memory required to store lower triangular elements of $\widetilde{\mathbf{K}}_{bb}$ is minimal. An algorithm for assembling, storing and solving a "partially symmetric" system like equation (10) is given by Zarco [12].

The global stiffness matrix can further be made fully symmetric by discarding the skew-symmetric part of $\hat{\mathbf{K}}$. The resulting symmetric stiffness matrix $\hat{\mathbf{K}}^s$ is given by:

$$\hat{\mathbf{K}}^s = \frac{1}{2}\left(\hat{\mathbf{K}} + \hat{\mathbf{K}}^T\right) \tag{12}$$

This technique for obtaining a symmetric boundary element stiffness matrix has been employed by Brebbia and Greorgiou, and Vallabhan et.al., and has been shown by Brebia [3] to correspond to a least squares approximation.

The proposed coupling method can easily be extended to the non-linear case. For a finite element formulation based on the Newton-Raphson method, the incremental displacements $\Delta\mathbf{U}^i$ for the i^{th} iteration is obtained by solving the system of equations:

$$\Delta\mathbf{U}^i = \left[\overline{\mathbf{K}}\left(\mathbf{U}^i\right)\right]^{-1} \mathbf{R}\left(\mathbf{U}^i\right) \tag{13}$$

where $\overline{\mathbf{K}}$ is the tangent stiffness matrix given by:

$$\overline{\mathbf{K}} = \frac{\partial \mathbf{R}}{\partial \mathbf{U}} \tag{14}$$

and $\mathbf{R}$ is the residual vector given by :

$$\mathbf{R} = \mathbf{KU} - \mathbf{F} \tag{15}$$

Solving for $\Delta\mathbf{U}^i$ from equation (13), the displacements for the i^{th} iteration of $\mathbf{U}^i$ can be obtained by:

$$\mathbf{U}^i = \mathbf{U}^{i-1} + \Delta\mathbf{U}^i \tag{16}$$

In most non-linear finite element computer programs, the tangent stiffness matrix and residual vector are computed for individual elements and then assembled to form the global tangent stiffness matrix and residual vector. For the boundary element system, the residual vector is given by:

$$\mathbf{R} = \hat{\mathbf{K}} + \hat{\mathbf{U}} - \hat{\mathbf{F}} \tag{17}$$

Since the far field is assumed to be linear, the equation $\hat{\mathbf{K}} + \hat{\mathbf{F}}$ is independent of $\hat{\mathbf{U}}$ and the tangent stiffness matrix for the boundary element system is simply equated to $\hat{\mathbf{K}}$. In assembling the tangent stiffness matrix, the same procedure for obtaining the system partitioned in the manner described in equation (10) is followed.

EFFECTS OF INFINITE BOUNDARY

To study the effects of the infinite boundary on the strip-footing problem, different methods for incorporating the infinite boundary into the finite element solution were investigated. These included (1) coupled boundary element-finite element method described in this study, (2) the analogue spring model, and (3) the use of infinite elements (Beer and Meek) [1]). In the coupled boundary element-finite element method, two analyses were performed to assess the effect of discarding the skew-symmetric part of the boundary element stiffness matrix. For all analyses, a 10 m. x 10 m. mesh was used. In the analogue spring model, the stiffness of the far field domain was approximated using a series of springs connected to the nodes located along the right-hand side and bottom boundary of the mesh. This is accomplished by imposing the mixed boundary conditions for every node located along the boundary.

Figure 2(a) shows the normalised relative vertical displacements along the surface versus the normalised co-ordinate *X/R* where $R = 10$m. is the domain size. When the analogue spring model is used, the underprediction in the vertical displacements with respect to the closed form solution for values of $X/R \leq 0.2$ is within 15%. Using infinite elements reduces this underprediction for $X/R \leq 0.2$ to within 10%. The coupled boundary element-finite element method results in vertical displacements which are within 0.5% of the closed form solution. This is true both for the case when the full stiffness matrix is used as well as when only the symmetric part is used.

Figure 2(b) shows the percentage error with respect to the closed form solution in the computed values of σ_{xx} along the diagonal. For the analogue spring model, errors in σ_{xx} as large as 40% occurring at $X/R = 0.4$ are observed. In general, the errors are larger than those in the conventional finite element analysis are where the infinite boundary is neglected and the displacements along the right-hand side and bottom boundary are fixed. Except for $X/R = 0.9$

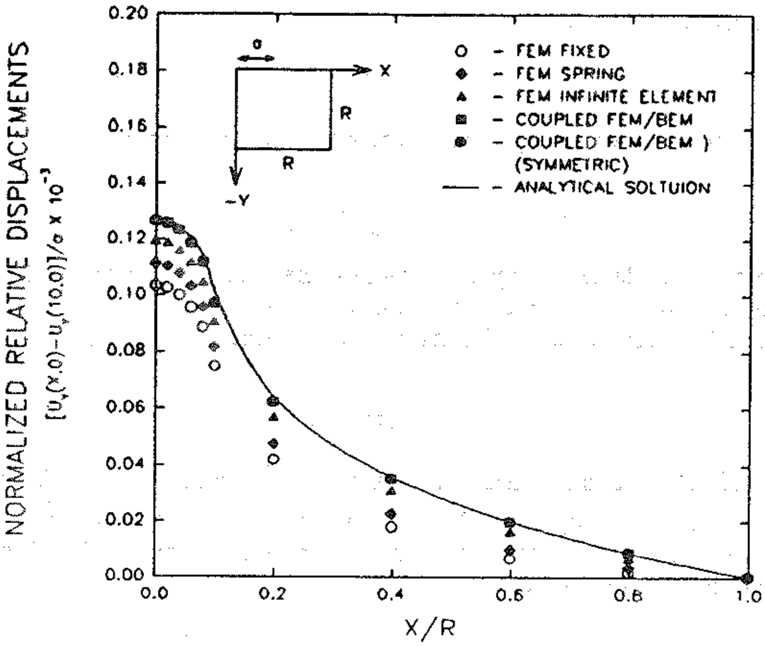

(a) Vertical displacements along surface

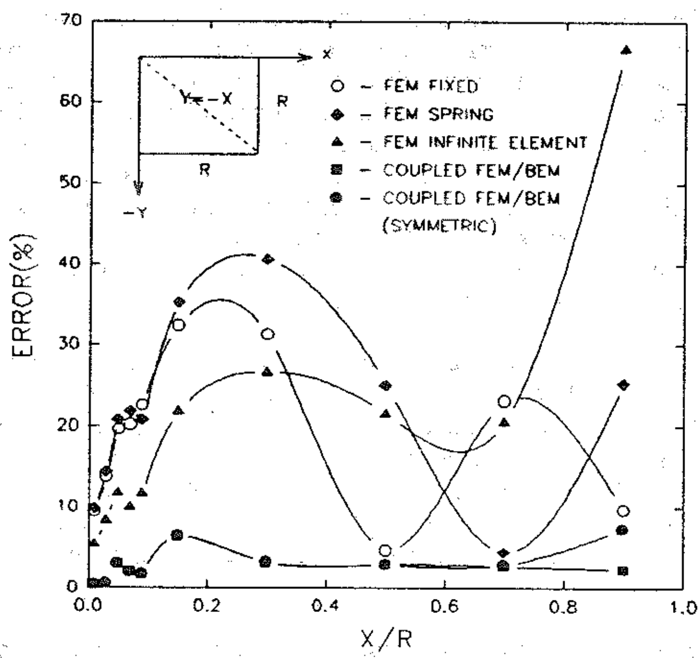

(b) σ_{xx} along diagonal elements

Figure 2. Effects of Infinite Boundary

where 68% error is observed, the use of infinite elements results in smaller errors in σ_{xx} as compared to the conventional finite element analysis. The coupled boundary element-finite element method results in values of σ_{xx} which are in general within 3% of the closed form solution. Except for the point X/R = 0.9, where the symmetric solution results in a slightly larger error, discarding the skew-symmetric part of the boundary element stiffness matrix does not have any significant effect on the value of obtained.

ELASTO-PLASTIC CASE

The homogeneous strip-footing problem was solved again assuming an elastic perfectly plastic material behaviour. A non-associated plasticity model assuming the Drucker-Prager failure criterion as the yield surface and the Von Mises failure criterion as the plastic potential function is implemented into a computer program BEFEC. Stresses are computed using a fully implicit integration scheme based on the radial return method (Wilkins, [11]). The consistent tangent formulation described by Simo and Taylor [8] is used together with the B method to compute the finite element tangent stiffness matrix. For the analysis performed, the same elastic parameters assumed in the homogeneous strip-footing problem are used. Also, it is assumed that the soil has a cohesion intercept of $c = 1.0$ kN/m^2, and was both frictionless ($\phi = 0°$) and weightless ($\gamma = 0.0$ KN/m^3).

The vertical displacement under the footing is measured relative to the edge point and normalised by the footing half-width a = 1.0 m., while the load w is normalised by c for values of $w/c \leq 3.0$, when the behaviour in both problems is elastic, the finite element solution gives displacements which are 20% beneath those of the coupled boundary element-finite element method. At $w/c \leq 4.0$, just after yielding has just begun to occur, the disparity in the vertical displacements computed using the two methods is reduced to 5%. However, as yielding progresses, the disparity between the two methods begins to increase again. The solution procedure progresses until $w/c \leq 5.2$ at which failure is predicted by both the finite element analysis as well as the coupled boundary element-finite element method. This result is close to the theoretical limit load $w/c \leq 5.14$ predicted by Prandtl. The most pronounce difference between the displacements obtained using the solution procedures occurs underneath the footing ($X/R \leq 0.1$) where the finite element analysis gives vertical displacements which are 20% below those obtained using the coupled boundary element-finite element method.

NONLINEAR U-FRAME LOCK CONSTRUCTION PROBLEM

This problem as illustrated in Figure 3(a) consists of a U-frame lock structure constructed on a clay foundation. Beside the lock, a 20ft. (6.1m.) high embankment with a slope 1:2.5 is built. Prior to the analysis, initial stresses in the soil due to self-weight are computed. The construction sequence involves first building the U-frame lock, after which the embankment is incrementally constructed in lifts. Lastly, the lock is filled to capacity with water. The construction of the U-frame lock is performed in a single load step by first assigning properties of fluid concrete to the element comprising the U-frame lock. In succeeding load steps, these elements are assigned the properties of hardened concrete to simulate the concrete setting. The embankment construction is performed using the "backfill placement" procedure. In this procedure, the elements comprising the embankment are assigned the properties of air. With each load step, a lift is placed by changing the properties of the elements in that lift from those of air to

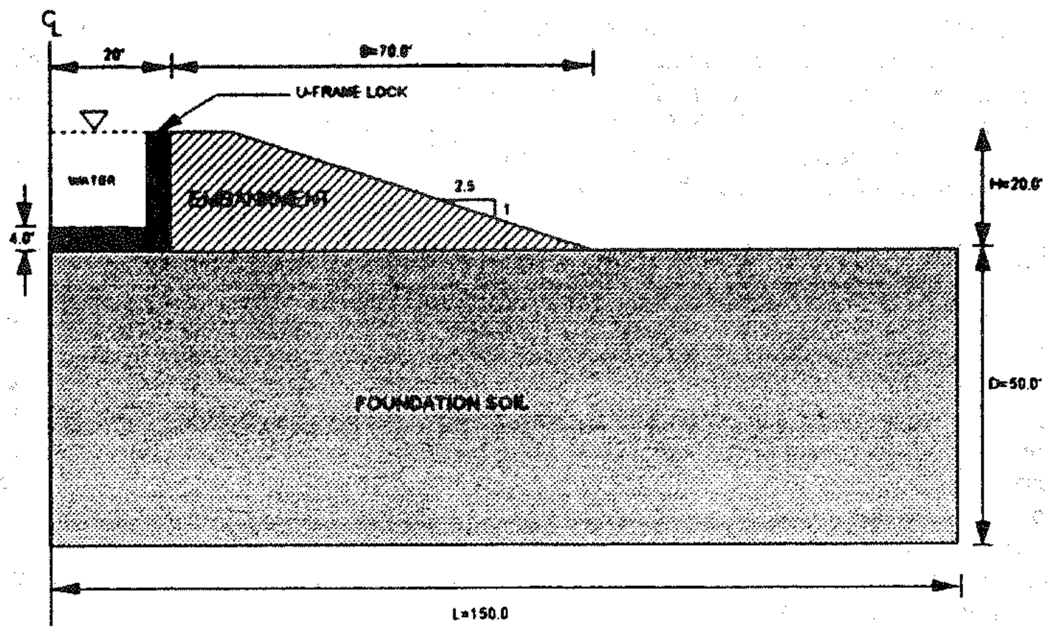

(a) Problem Geometry

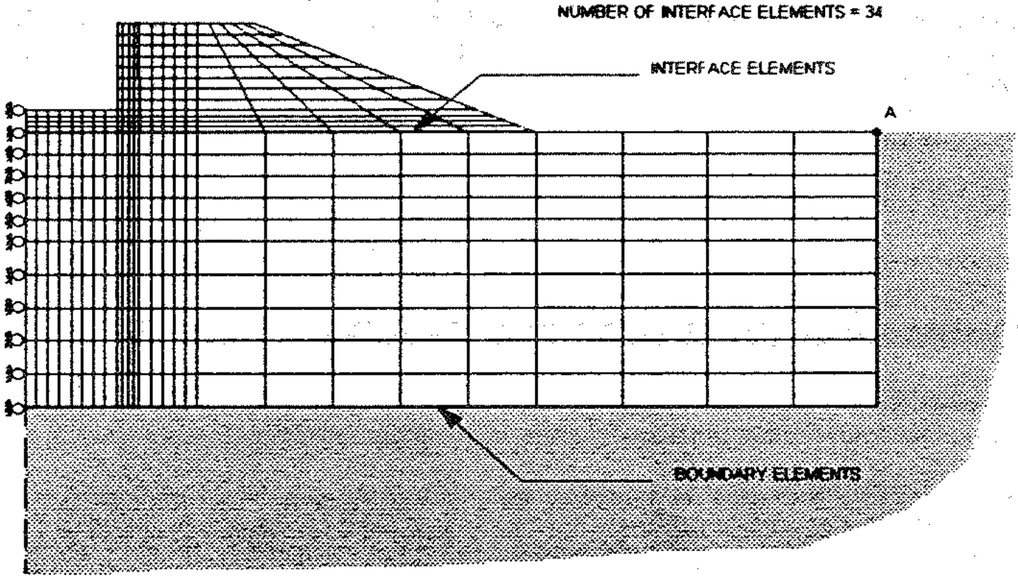

(b) Coupled boundary element-finite element mesh used to model problem

Figure 3. U-frame lock construction problem

soil. When the elements within each lift first placed, they are assigned the properties of a dense fluid with a low modulus. In subsequent load steps, these elements are allowed to harden by assigning the modulus of soil to them.

In the analyses performed, the embankment is constructed in 10 lifts each lift being 2 ft. (0.61m) high. The U-frame lock is assumed linearly elastic with E = 4.5 x 10^8 psf (21.5 GPa), ν = 0.2, and γ = 150 pcf (23.7 kN/m^3). The soil in the foundation and embankment is assumed to behave according to the hyperbolic stress-strain model (Duncan and Chang, [4]). A summary of the material parameters assumed for the hyperbolic model are given in Table 1. To model the relative movement between the different materials, interface elements (Goodman, Taylor and Brekke, [5] are used. These elements are placed along the interfaces between the lock and foundation, lock and embankment, and foundation and embankment. A bilinear material behaviour was assumed for the interface elements.

Table 1. Material parameters for soils in U-frame lock problem (Non-linear case)

Material Parameter	Foundation	Embankment
Modulus number, K	340	300
Modulus exponent, n	0.011	0.5
Failure ratio, R_f	0.8	0.8
Cohesion intercept, c	1000 psf	400 psf
Friction angle, ϕ	0.0 deg	37.0 deg
Unit weight, Υ	125 pcf	25 pcf
Coefficient of lateral earth pressure at rest, K_o	1.0	0.5
Poison's Ratio, υ	0.49	0.3

Table 2. Material parameters for interface elements in nonlinear U-frame lock problem

Material Parameter	Lock-Foundation	Lock-Embankment	Foundation-Embankment
Shear Stiffness K_s (psf)	36000	6000	36000
Normal Stiffness K_s (psf)	1 x 10^8	1 x 10^8	1 x 10^8
Minimum Shear Stiffness (psf), K_s	100	100	100
Minimum Normal Stiffness (psf), K_s	100	100	100
Cohesion, c (psf)	1000.0	0.0	1000.0
Friction angle, ϕ	0.0 deg	17.0 deg	0.0 deg

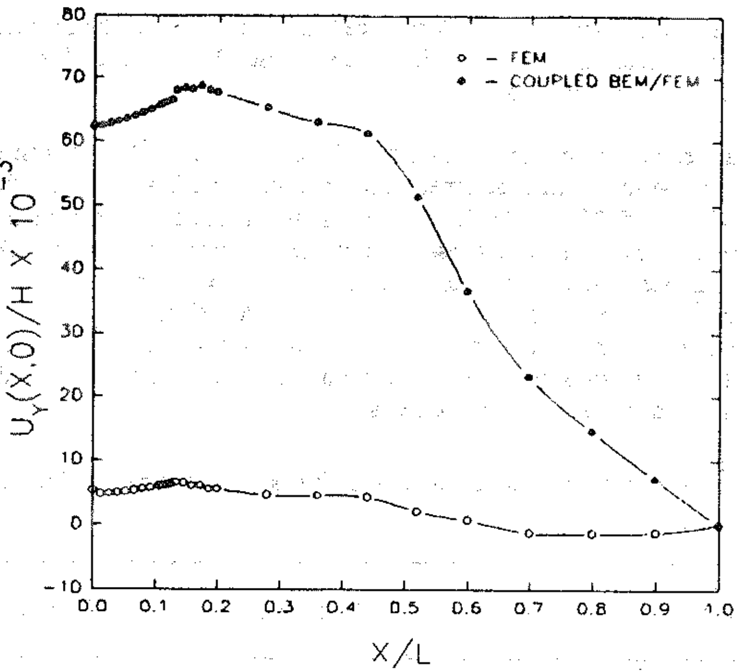

(a) Vertical displacements along surface

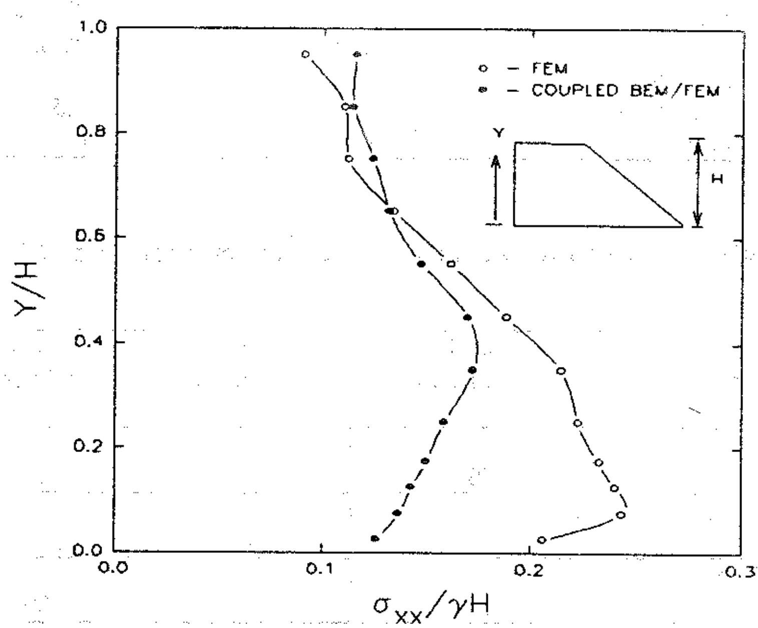

(b) Lateral earth pressures exerted against lock wall

Figure 4. U-frame lock problem results

Table 2 gives a summary of the material parameters assumed for the interface elements. The effects of the infinite boundary are investigated by performing two analyses. In the first analysis, the problem is solved using only the finite element method, while the coupled boundary element-finite element method is used in the second analysis.

Figure 3(b) illustrates the mesh used in the coupled boundary element-finite element analysis. In this mesh, the point labelled *A* is located on the foundation surface 150.0-ft. (45.7 m.) from the centreline is used as a reference point for measuring all displacements. A similar mesh with a reference point for measuring all displacements. A similar mesh with the displacements along the right-hand side and bottom boundary fixed was used in the finite element analysis. For the far field in the coupled solution, it was assumed that $E = 1.5 \times 10^6$ psf (71.8 MPa), $\nu = 0.495$. This value of E was obtained by averaging the tangent moduli along the bottom boundary of the boundary based on the initial stress analysis.

Figure 4(a) shows the vertical displacements along the surface, measured relative to point *A* and normalised by the embankment height *H*, versus the normalised co-ordinate *X/L* where L = 150 ft. (45.7 m.) is the length of the foundation domain. This figure shows that for all values of $X/L \leq 10$, taking into account the effects of the infinite boundary results in a ten-fold increase in the computed vertical displacements as compared to the case where these effects are ignored. This disparity is much greater than that observed in the strip-footing problem and can be explained by the fact that the loaded area to the depth of the foundation domain in this problem is significantly greater than that in the strip footing problem.

Figure 4(b) shows the lateral earth pressures exerted by the embankment on the lock wall. In this figure, the lateral pressure is normalised by the quantity γH where $\gamma = 125$ pcf (19.8 KN/m^3) is the unit weight of the embankment soil and is plotted versus the normalised co-ordinate *Y/H* where *Y* is the distance from the base of the embankment. For values of $Y/H > 0.7$, the coupled boundary element-finite element method results in lateral earth pressures which are as much as 15% greater as compared to those obtained using the finite element method only. For values of $Y/H < 0.7$, the finite element analysis gives values of lateral earth pressure which are significantly greater than those obtained using the coupled boundary element-finite element method. The disparity is most significant for $Y/H \leq 0.3$ where the finite element analysis gives lateral earth pressures that are double those obtained from the coupled boundary element-finite element method.

CONCLUSIONS

A method for solving soil-structure interaction problems that includes the infinite-boundary effects of the far field domain was developed. The method involved coupling boundary elements based on the Melan solution with finite elements in a manner so as to result in a system of equations which is both symmetric and banded. For the elastic strip-footing problem, it was noted that neglecting the effects of the infinite boundary resulted in errors in the displacement and stresses as large as 20% and 30% respectively when compared with the close form solution. These errors were observed to decrease with increasing domain size and were unaffected by the type of finite elements used as well as the type of boundary condition assumed on the right-hand side boundary. Simulating the infinite domain using the analog spring model or infinite elements decreased the errors occurring in the displacements but affected the errors in the stresses. Using the proposed coupling method resulted in displacements and stress within 3% of the closed form solution. For the elasto-plastic strip footing, the infinite boundary resulted in vertical displacements which were 20 neglecting the far field. For the nonlinear U-frame lock construction problem, taking into consideration the effects of the infinite boundary resulted in a ten-fold increase in the vertical displacements as compared to the finite element analysis. The infinite boundary also resulted in lateral earth pressures against the lock which were half of those obtained when the far field was neglected.

ACKNOWLEDGMENTS

Funding for this study was provided by the US Army Engineers Waterways Experiment Station (WES) under Contract No. DACW39-91-C-0085.

REFERENCES

[1] C. Beer and J. L. Meek (1977). Infinite domain elements. International Journal of Numerical Methods in Engineering, vol 11, pp. 53-64.

[2] C. A. Brebbia and P. Georgiou (1979). Combination of boundary and finite elements is elastostatics. Applied Mathematical Modelling, vol.3, pp. 212-220.

[3] C. A. Brebbia and J. C. F. Telles, and L. C. Wrobel (1984). Boundary Element Techniques in Engineering. Springer - Verlag, New York.

[4] J. M. Duncan and C. Y. Chang (1970). Nonlinear analysis of stress and strain in soils. Journal of Soil Mechanics and Foundations Division, ASCE, 96 (SM5, Proc. Paper 7513), pp. 1629 - 1653.

[5] R. E. Goodman, R. L. Taylor, and T. L. Brekke (1968). A model for the mechanics of jointed rock. Journal of Soil Mechanics and Foundations Division, ASCE, 94 (SM3, Proc. Paper 5937), pp. 637-659.

[6] J. Jirousek and P. Teodorescu (1982). Infinite domain elements. Computers and Structures, vol. 15, pp. 575-587.

[7] C. Johnston and J. C. Nedelec (1980). On coupling the boundary integral and finite element method. Math. Comp., vol. 35, pp.1063 -1079.

[8] J. C. Simo and R. L. Taylor (1986). Consistent tangent operators for rate-independent elastoplasticity. Computational Methods in Applied Mechanics, vol. 23, pp. 239-252.

[9] J. C. F. Telles and C. A. Brebbia (1981). Boundary element solution of half-plane problems. International Journal of Solids and Structures, vol. 18, pp. 1149-1158.

[10] C. V. G. Vallabhan, J. Sivakumar, and N. Radhakrishnan (1986). Applications of boundary element method for soil-structure interaction problems. In Proc. 6th International Conference on Boundary Element Methods, vol. 6, pp. 67-79.

[11] M.L.Wilkins (1964). Methods in Computational Physics, vol. 3, chapter Calculations of Elastic-Plastic Flow. Academic Press, New York.
[12] M. A. Zarco (1993). Solution of Soil-Structure Interaction Problems by Coupled Boundary Element-Finite Element Method. PhD. Thesis, Virginia Polytechnic Institute and State University.
[13] A. P. Zielinski and O. C. Zienkiewicz (1985). Generalized finite element analysis with T complete boundary solution functions. International Journal of Numerical Methods in Engineering, vol. 21, pp. 509-528.
[14] O. C. Zienkiewicz, D. W. Kelley, and P. Bettess (1977). The coupling of the finite element method and boundary element solution procedures. International Journal of Numerical Methods in Engineering, vol. 11, pp. 355-375.